ISSN : 0974-7419 Volume 11 Issue 6

Trade Science Inc.

Analytical CHEMISTRY

An Indian Journal

Full Paper

ACAIJ, 11(6) 2012 [231-239]

Physico-chemical properties of activated carbons prepared from almond shell: Application for the removal of total organic carbon from Tunisian industrial phosphoric acid

Abdessalem Omri[1]*, Mourad Benzina[1], Wassim Trabelsi[2]

[1]Laboratory of Water-Energy-Environment (LR3E), code: AD-10-02, National School of Engineers of Sfax, University of Sfax, BP W, 3038 Sfax, (TUNISIA)

[2]Groupe Chimique Tunisien, route de Gabès km 3,5, Sfax – Tunisie, B.P- 393/3018, (TUNISIA)

E-mail: omriabdesslem@yahoo.fr

Received: 21st February, 2012 ; Accepted: 21st March, 2012

ABSTRACT

Activated carbons were prepared through physical activation of almond shell precursor, using carbon dioxide as the physical agent. The effects of the preparation variables, such as activation temperature, carbon dioxide flow rate and activation time, on the adsorption capacity of iodine and methylene blue solution were investigated. The activated carbon which had the highest iodine and methylene blue numbers was obtained by these conditions as follows: 800 °C activation temperature, 100 cm^3/min carbon dioxide flow rate and 120 min activation time. The characterization of carbon materials is performed by scanning electron microscopy (SEM), X-ray diffraction (XRD), Fourier transform infrared spectroscopy (FTIR), ^{13}C (CP/MAS and MAS) solid-state NMR, nitrogen adsorption (BET) and Boehm's titration method. For the determination of the adsorptive capacity of the activated carbon, removal of total organic carbon from Tunisian industrial phosphoric acid was carried. Experimental results showed that TOC could be adsorbed effectively by the oxidized almond shell-activated carbon. The eliminatory capacity of these activated carbons was comparable with those of some commercial activated carbons.

KEYWORDS

Almond shell;
Activated carbon;
Physico-chemical properties;
Oxidation;
Total organic carbon.

INTRODUCTION

Activated carbons with high surface area and pore volumes are produced from a variety of carbonaceous raw materials. In practice, coal and agricultural by-products or lignocellulosic materials are two main sources for the production of commercial activated carbons. In recent years, condensed research has been reported on the production of low cost activated carbon from agricultural residues such as olive-waste cakes[1], corncobs[2], Tamarind wood[3], pecan shell[4], coconut husk[5], palm shell[6], coffee grounds[7], almond husk[8], and corn[9]. In principle, the activation methods can be divided into two categories: chemical and physical activation. In a chemical activation, the raw material is impregnated with an activating reagent like $ZnCl_2$, H_3PO_4, KOH and K_2CO_3 or their mixtures[10-12]. In physical activation, a raw material is first carbonized, and the

resulting char is secondarily activated under a flow of suitable gas such as carbon dioxide, steam, air or their mixtures[13-15]. The physical preparation process using carbon dioxide was investigated in this study.

The physical properties and the chemical composition of the precursor, as well as the methods and process conditions employed for activation, determine the final pore size distribution and the adsorption properties of the activated carbon[16]. This effective adsorbent is used for the separation and removal of unwanted matters from industrial effluents. It finds wide application in food, pharmaceuticals, solvent recovery, drinking water treatment, fuel cells, chemical and other process industries[17].

The aims of this work were to utilize almond shells for the preparation of activated carbon by simple thermo-physical activation using CO_2 as an activating agent. At present, this agricultural waste material is used principally as a solid fuel and is available in abundance in Sfax, Tunisia. This prepared activated carbon was used for the elimination of the total organic carbon contained in Tunisian industrial phosphoric acid manufactured from phosphate rock by the SIAPE society using wet process[18]. In this study, the effects of activation temperature, carbon dioxide flow rate and activation time on iodine and methylene blue numbers of the activated carbon were studied in order to obtain high adsorption capacity and surface area of the product. Subsequently, the physico-chemical characteristics of the activated carbon, obtained by optimum conditions, were also determined.

EXPERIMENTAL

Preparation conditions of activated carbons

Almond shell was obtained from the local market in Sfax, Tunisia. Almond shell was firstly washed and subsequently dried at 105 °C for 24 h to remove the moisture content. The dried samples were ground and sieved to the size of 1–2 mm. Carbonization of the raw shells and activation of the resulting chars were both carried out in a vertical stainless-steel reactor, which was placed in an electrical furnace Nabertherm. During the carbonization process, about 15 g of raw material was used to prepare the chars. Nitrogen gas at a flow rate of 150 cm^3/min was passed through the reactor right from the beginning of the carbonization process. The furnace temperature was increased at a rate of 5 °C/min from room temperature to 450 °C and held at this temperature for 1 h. After pyrolysis, the furnace was cooled down to room temperature with N_2 flushing through the sample. The resulting chars were then activated by a CO_2 flow to prepare for the final product at fixed heating rate at 10 °C/min. For the activation process, the effects of activation temperature, activation time and carbon dioxide flow rate were studied to obtain the optimum conditions for the process.

Optimum conditions for the production of activated carbon

Some parameters which had effect on the activated carbon namely impregnation ratio of activation temperature (600–900 °C), activation time (30 –120 min) and carbon dioxide flow rate (50–200 cm^3/min) were studied to determine the optimum conditions for producing this activated carbon. In this work, efficiency and quality of the activated carbon were preliminarily characterized by measuring both iodine number and methylene blue number. Iodine number can be used for estimation of the relative surface area and measurement of porosity, the pores size greater than 1.0 nm in diameter. Therefore, the iodine number was measured to evaluate the adsorptive capacity of the produced activated carbon. In case of methylene blue number, it is also one of the most widely recognized probe molecules for assessing the removal capacity of the specific carbon for moderate-size pollutant molecules (=1.5 nm)[19].

(A) Adsorption of iodine

The iodine number of activated carbon was obtained on the basis of the Standard Test Method, ASTM Designation D4607- 86 by titration with sodium thiosulphate (ASTM, D 4607-86). The concentration of iodine solution was thus calculated from total volume of sodium thiosulphate used and volume dilution factor.

(B) Adsorption of methylene blue

Methylene blue adsorption was conducted by mixing 0.2 g of the prepared activated carbon with 100 mL of 1000 mg/L methylene blue solution[20]. After agitation during 24 h, the suspension was filtered and the methylene blue residual concentration was measured at 660 nm, using an UV/vis spectrophotometer (Visible

spectrophotometer 1011, CECIL). A previously established linear Beer-Lambert relationship was used for the concentration determination.

Characterization of the prepared activated carbon

(A) Textural characterization

Textural characteristics were determined by nitrogen adsorption at -196 °C with an automatic adsorption instrument (TriStar 3000 V6.04 A, Micromeritics). Prior to the measurements, the samples were out gassed at 300 °C under nitrogen for at least 24 h. The amount of N_2 adsorbed at relative pressures near unity (~0.99) corresponds to the mole number of adsorbed nitrogen per gram of activated carbon. The surface area of the sample was calculated by Brunauer-Emmet-Teller (BET) method in relative pressure (P/P_0) range of 0.05-0.30 at -196 °C. In addition, a scanning electron microscopy (Philips XL30) was used to visualize morphology of the raw material (almond shell) and the activated carbon prepared in the optimal conditions.

(B) Chemical characterization

The surface organic functional groups and structure were studied by FTIR spectroscopy. The FTIR spectra of the raw material and the resulting activated carbon were recorded between 500 and 4000 cm^{-1} in a NICOET spectrometer.

The well-known Boehm's method allows modeling the principal acidic oxygenated functions of the activated carbon such as carboxylic acids, lactones and phenols using bases of increasing strength as $NaHCO_3$, Na_2CO_3 and NaOH, respectively. Then, the total basicity is given by titration by HCl. More details are given in Refs.[21,22].

The NMR spectrum was recorded in a Bruker (300 MHz) spectrometer operating at a carbon resonance frequency of 75.467 MHz and at 20 °C. ^{13}C cross-polarization magic-angle spinning (CP/MAS) and magic-angle spinning (MAS) were used to characterize the optimal activated carbon.

The surface of inorganic components were analyzed by an X-Ray diffractometer a Philips® PW 1710 diffractometer (Cu Kα, 40 kV/40 mA, scanning rate of 2θ per min).

(C) TOC removal test

The industrial acid solution used was a 54% P_2O_5 (about 9M H_3PO_4) solution containing an initial concentration of Total Organic Carbon (COT) equalizes with 578 ppm. The removal of TOC was carried out in the following manner: a known amount of prepared activated carbon was placed in Erlenmeyer flasks of 250 ml capacity in contact with 100 g of industrial phosphoric acid solutions at a certain temperature (40– 60 °C). A reflux refrigerant is placed on each Erlenmeyer to avoid water evaporation. After contact desired time, carbon particles and the supernatant acid were separated by filtration on an organic membrane of convenient porosity. TOC was determined by a Shimadzu TOC-5050 apparatus.

RESULTS AND DISCUSSION

Optimum conditions for the production of activated carbon

(A) Activation temperature

Activation temperature was shown to have remarkable effects on both surface area and the nature of porosity. The increase in temperature would release increasing volatiles as a result of intensifying dehydration and elimination reaction and also increased the $C–CO_2$ reaction rate[23,24]. Enhance activation temperature significantly enhanced of both micro-and mesopore developments, resulting in the increase of both iodine and methylene blue adsorptive capacities of the activated carbon. From the results as shown in Figure 1, it illustrated that starting from 800°C the prepared activated carbon have high iodine and methylene blue numbers at constant activation time of 2 h and carbon dioxide flow rate equal to 100 cm^3/min. Additionally, the yield of activated carbon defined as the ratio of the mass of activated carbon produced upon the mass of the raw material used, was decreased for the activation temperature increases from 600 to 900°C (TABLE 1). This is attributed to the removal of volatile matters resulting from the decomposition of major compounds of almond shell i.e. cellulose (long polymer of glucose without branches) and hemicellulose (constituted of various branched saccharides)[25].

Above 800 °C, the yield becomes constant because all cellulose and hemicellulose are decomposed. It remains lignin, the third component of almond shell, the

decomposition of which is more difficult. Thus, at 800 °C was chosen as the optimum activation temperature.

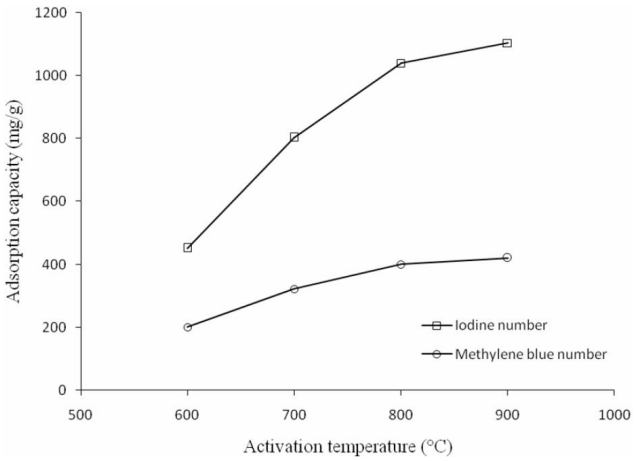

Figure 1 : Effect of activation temperature on iodine and methylene blue numbers of optimal activated carbon.

TABLE 1 : Effect of activation temperature on the yield of activated carbon

Temperature (°C)	Yield (%)
600	29.75
700	24.61
800	23.47
900	23.29

(B) Activation time

The effect of activation time on iodine and methylene blue number was studied by varying the time from 30 to 120 min at constant activation temperature of 800°C and carbon dioxide flow rate about to 100 cm^3/min. Figure 2, shows that increasing of activation time resulting in the increase of the iodine and methylene blue numbers. The results present that 120 min is the suitable length of time for activation because it gave the highest iodine and methylene blue numbers of product with a maximum value of 1060.43 mg/g and 414.78 mg/g, respectively. This trend is expected because some volatile compounds which were in the inner part of particle could evaporate more with long activation. The reason is that heat penetrated deeper inside of particles than at short time, so the porosity development at long time was higher than at short time resulting in the increase of iodine number[26].

(C) Carbon dioxide flow rate

The effect of carbon dioxide flow rate on the iodine and methylene blue number is given in Figure 3. Increasing the CO_2 flow rate from 50 to 100 cm^3/min increases the adsorption capacity of the activated carbons for the molecules of iodine and methylene blue. This means that, at a flow rate of 50 cm^3/min, the carbon burnoff due to carbon–CO_2 reaction is not sufficiently high to maximize the BET surface area in the activated carbons. At 50 cm^3/min, it is also possible that the volatiles released from the samples might not be completely entrained in the low-velocity CO_2 flow but be deposited on the sample surface again, thereby hindering pore development[27]. At a flow rate of 100 cm^3/min, the iodine and methylene blue numbers are maximum values. For flow rates of 150 cm^3/min and greater, the higher flow velocities above that for 100 cm^3/min reduce the contact time between the CO_2 molecules and the sample surface and thereby decrease the diffusion of the molecules into the pore structures and hence reduced adsorption capacity was obtained.

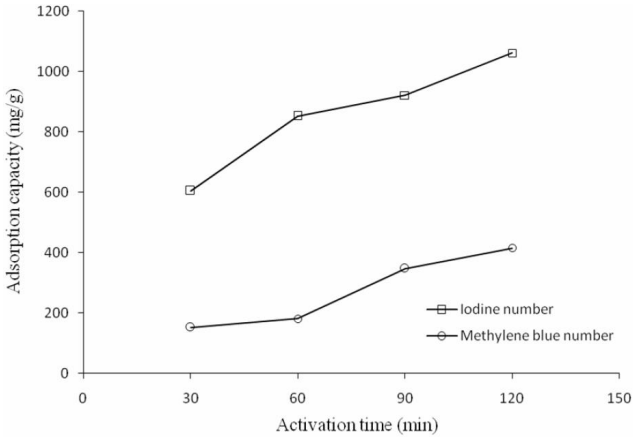

Figure 2 : Effect of activation time on iodine and methylene blue numbers of optimal activated carbon.

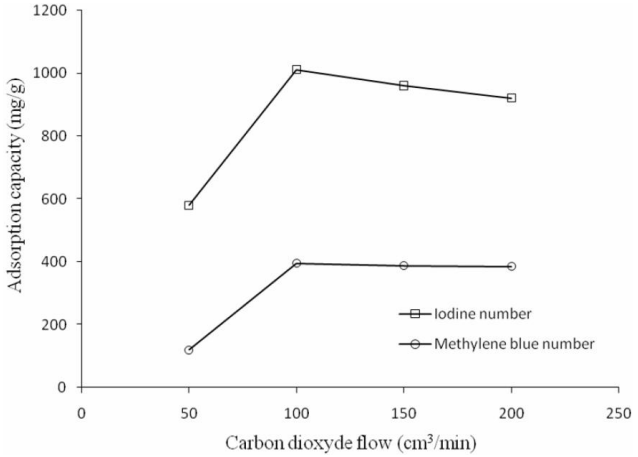

Figure 3 : Effect of carbon dioxide flow rate on iodine and methylene blue numbers of optimal activated carbon.

Note that all experiments were conducted in optimal conditions of activation temperature and contact time.

Characterization of the optimal activated carbon

According to Section 3.1, optimized conditions were selected as activation temperature at 800 °C, a carbon dioxide flow rate of 100 cm^3/min and an activation time equal to 120 min. Figure 4 shows nitrogen adsorption/desorption isotherm curve onto the activated carbon prepared at optimized conditions at -196 °C. The obtained isotherm curve belongs to a mixed type in the IUPAC classification, type I at low pressure and type IV at intermediate and high P/Po. In the initial part, they are type I, with an important uptake at low relative pressures, the characteristic of microporous materials. However, the open knee is presented, no clear plateau is attained and certain slope can be observed at intermediate and high relative pressures. All these facts indicate the transition from microporosity to mesoporosity (type IV). Additionally, a desorption hysteresis loop due to adsorbate condensation in the mesopores is presented. The adsorption isotherm of this material showed a good agreement with those reports in the literatures[28,29].

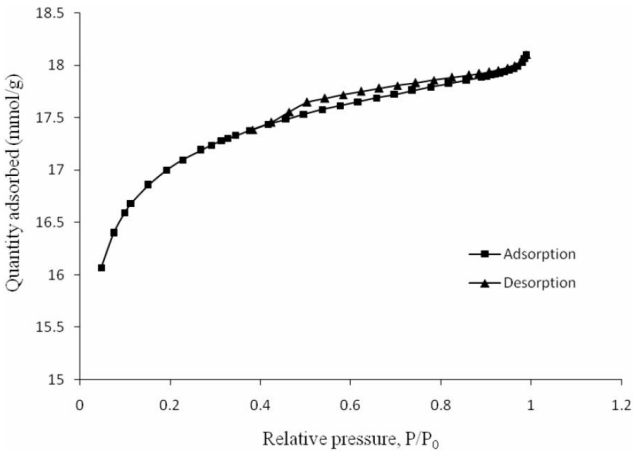

Figure 4 : Nitrogen adsorption–desorption isotherms of optimal activated carbon.

Microstructure of the resulting activated carbon prepared in the optimal conditions in Figure 5 shows that the adsorbent gives roughly texture with heterogeneous surface and a variety of randomly distributed pore size. Furthermore, it contains an irregular and highly porous surface, indicating relatively high surface area. This observation can be supported by BET surface area of the prepared activated carbon as illustrated in TABLE 2.

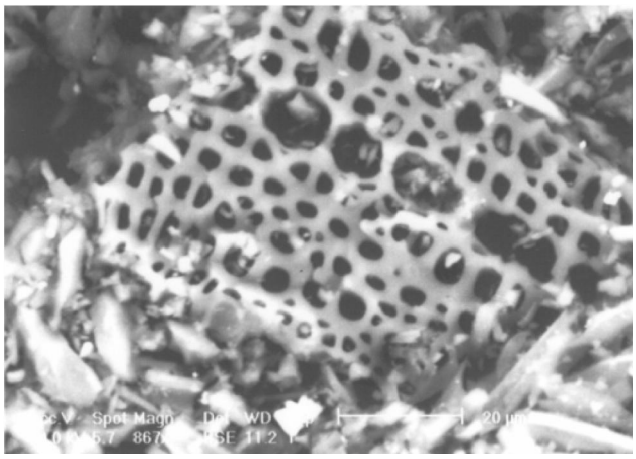

Figure 5 : SEM image of resulting activated carbon.

TABLE 2 : Surface area, quantity adsorbed of nitrogen and pose size.

Parameters	Values
BET surface area, S_{BET} (m^2/g)	1310.134
quantity adsorbed of nitrogen (mmol/g)	13.422
Average pore diameter (Å)	19.58

For this activated carbon prepared under optimized condition, the X-ray diffraction profiles shown in Figure 6 exhibit broad peaks and absence of a sharp peak that revealed predominantly amorphous structure, which is an advantageous property for well-defined adsorbents. However, the occurrence of broad peaks around 25° and 43° showed signs of formation of a crystalline carbonaceous structure, resulting in better layer alignment[30]. Similar result reported was proposed by Pechyen et al.[31].

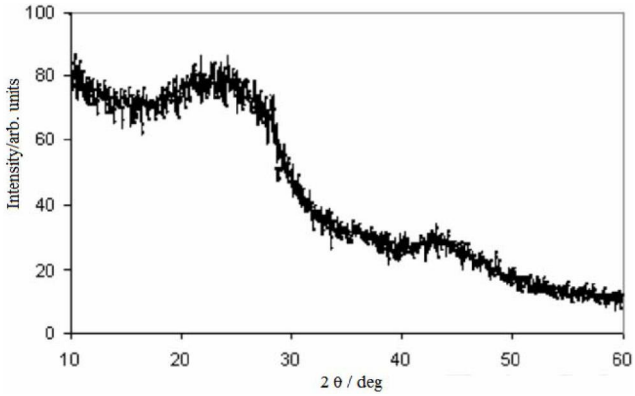

Figure 6 : X-ray diffraction profile of optimal activated carbon.

The analysis of surface functions covered the carbons made it possible to identify the whole of the acid and basic groupings. Some examples of oxygen con-

Full Paper

taining functionalities detected on the carbon surface include the following: carboxylic, lactone, phenol, carbonyl, pyrone, chromene, quinone, and ether groups (Figure 7)[32]. The results of analysis the surface oxygen functional groups of our activated carbon product carried to the TABLE 3, make it possible to note that the quantity of the acid functions is much more important than those of the basic functions. So we can conclude that the activated carbons are of type acids.

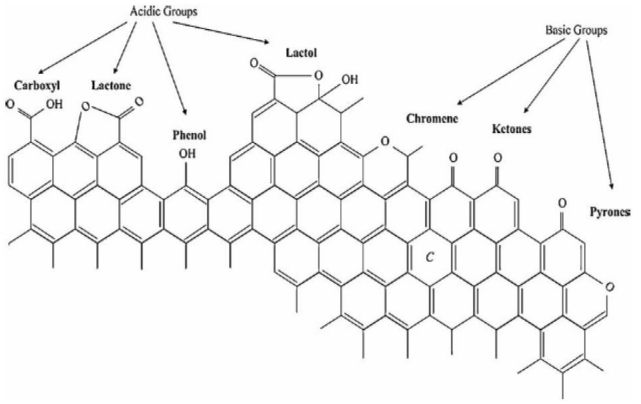

Figure 7 : Acidic and basic surface functionalities on a carbon basal plane[32].

TABLE 3 : Concentrations (meq/g) of acidic and basic groups of the surface in optimal activated carbon

Surface functions	Values
Total of acid functions	**2.606**
Carboxylic (-COOH)	1.604
Lactones (-COO-)	0.875
Phenol (-OH)	0.127
Total of basic functions	**1.598**

The solid-state ^{13}C NMR spectrum of produced activated carbon shows that the lignocellulosic structures were completely transformed into a polycyclic material with the preponderance of heteroaromatic structures, as indicated by the signal observed in the 110-130 ppm region (Figure 8). Aromatic groups present in the lignin favor re-ordering of elemental carbon upon a possible thermal treatment. In addition, the signal in at 125 ppm indicates the presence of benzene groups associated with these basal planes.

Additionally information about the chemical structure and functional groups, infrared spectroscopy of the prepared activated carbon was studied in this work. It is noted that the infrared spectroscopy of the raw material (almond shell) was analyzed in my preceding work[32]. The spectrum of the optimal adsorbent prepared is given in Figure 9. The band located at 3447 cm^{-1} is attributed to ν (O–H) vibrations in hydroxyl groups. The weak and broad peaks that appear at 2254 cm^{-1} could be assigned to ν (C=C) vibrations in alkyne groups. The skeletal C=C vibrations in aromatic rings cause the absorptions in 1585 cm^{-1}. The absorptions at 1438 cm^{-1} could be the result of C–O stretching in carboxylate groups. The peaks at 1130 cm^{-1} are due to the vibrations of C–O stretching. The C–H out-of-plane bending in benzene derivative vibrations causes the band at 890 cm^{-1}[1].

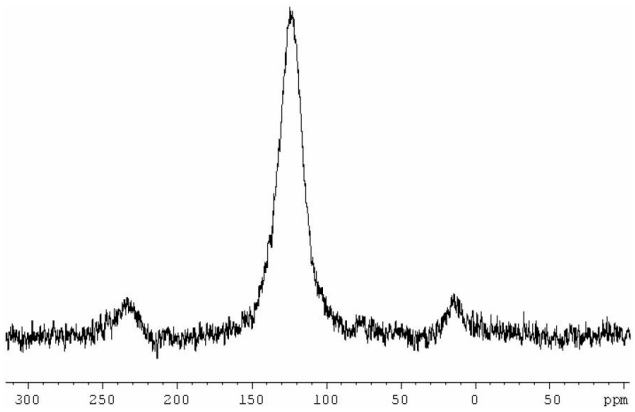

Figure 8 : Solid-state ^{13}C NMR spectrum of produced activated carbon.

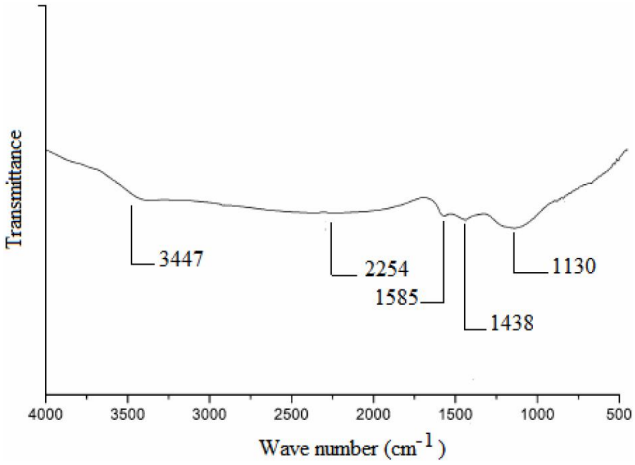

Figure 9 : FT-IR spectra of optimal activated carbon.

APPLICATION OF OPTIMAL ACTIVATED CARBON TO THE REMOVAL OF TOTAL ORGANIC CARBON CONTAINED IN TUNISIAN INDUSTRIAL PHOSPHORIC ACID

Activated carbon prepared from almond shell

at optimum conditions is characterized by an acidic surface. Considering that the majority of organic matter contained in industrial phosphoric acid is the acid type (di-n-bytul phthalate, humic acid and fulvic acid)[33,34], it is necessary to modify surface of the activated carbon to make it more alkaline.

Modification of the surface chemistry of carbons

(A) Ammoxidation of the resulting activated carbon

The objective of ammonxidation is to increase the basicity of activated carbon by introducing basic nitrogen functionalities to the carbon surface[35,38]. Apart from the incorporation of basic nitrogen functionalities during heat treatment under ammonia flow, the removal of oxygen containing functionalities can significantly improve the basicity of ammonia treated carbons[35,39]. In the reaction with ammonia at elevated temperatures ether-like oxygen surface groups are easily replaced by –NH– on the carbon surface that through dehydrogenation reaction could readily lead to imine and pyridine functionalities as shown in Figure 10[40].

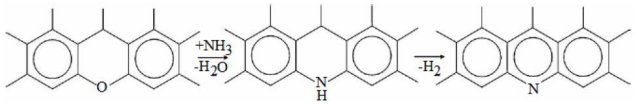

Figure 10 : Reaction scheme for conversion of chemisorbed oxygen (ether-like) into imine and pyridine surface groups in the reaction with ammonia[41].

The ammoxidation was performed on a glass sintered inside a glass tube reactor where a flow of air and ammonia circulates. A mass of activated carbon equal to 10 g is used to avoid large differences in terms of ammoxidation degree. The flows of the air and the ammonia are 6000 and 1200 ml/h, respectively, controlled with two rotameters. This apparatus is then introduced in a circular furnace for 6 h at a fixed temperature of 400 °C. The power of heating is controlled with a thermocouple that is in contact with the surface of the sample. After reaction, the removed sample is mixed and placed in a dessicator under vacuum at 110 °C. To complete the elimination of ammonia, the activated carbon is washed with 2000 ml of distilled water under agitation for 24 h and then dried at 110 °C.

(B) Effect of ammoxidation on the surface functions

The distribution of acid groups and the basic group is detailed in histogram (Figure 11). One can note first of all, for the ammoxidated samples, an expected increase in the total basicity occurs. Secondly, the phenols and the lactones undergo a decrease in their concentration. The amount of carboxylic acids decreases also but more slightly. Lactones are cyclic esters, thus they could react easily with ammonia to give amide groups. The carboxylic acids could also react with ammonia giving the same nitrogenated functions according to the following reaction[41]:

$$-COO^{-}NH_4^{+} \xrightarrow{-H_2O} -CO-NH_2 \xrightarrow{-H_2O} C \equiv N \quad (1)$$

Moreover, some dihydroxy-phenols became quinones by both effects of the oxygen and the high temperature[42]:

$$-OH + NH_3 \longrightarrow -NH_2 + H_2O \quad (2)$$

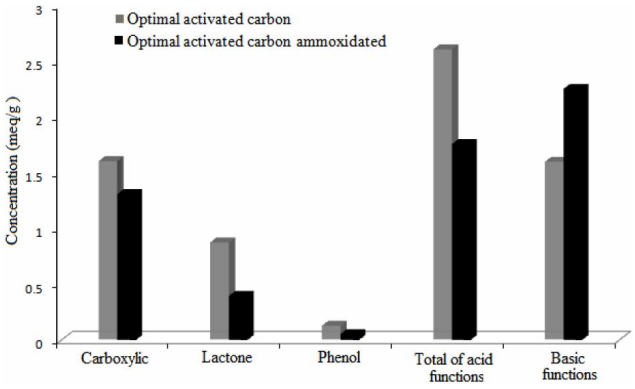

Figure 11 : Concentrations of the acid and basic groupings for the surface of optimal activated carbon.

TOC removal tests

Figure 12 shows the effects of specific consumption on the removal of TOC contained in industrial phosphoric acid at various temperatures onto the ammoxidated activated carbons prepared at optimal conditions. The specific consumption was calculated by using the following equation,

$$\text{Specific consumption} = \frac{m_{AC}}{m_{P_2O_5}} \quad (3)$$

and the removal efficiency of TOC was calculated as follows:

$$\%\ \text{Removal of TOC} = \frac{TOC_0 - TOC_r}{TOC_0} \times 100 \quad (4)$$

Where m_{AC} is the mass of the activated carbon (g), m_{P2O5} is the mass of P_2O_5 contained in industrial phosphoric acid (kg), TOC_0 and TOC_r are the concentrations of Total Organic Carbon initial and residual, re-

spectively. The specific consumption is an important parameter because this parameter determines the capacity of adsorbent for a given TOC concentration and also determines sorbent–sorbate equilibrium of the system. The increased removal at high consumption of activated carbon is expected, because of the increased adsorbent surface area and availability of more adsorption sites[42,43]. The optimum specific consumption was found to be 16 g AC/kg P_2O_5. From the figure 12, the removal of TOC was increases with temperature, which indicates the endothermic nature of the adsorption reaction. At higher temperature, more organic molecules have sufficient energy to undergo an interaction with active sites at the surface. In addition, increasing the temperature was known to increase the rate of diffusion of the adsorbate molecules across the external boundary layer and in the internal pores of the adsorbent particle due to the decrease in the viscosity of the solution[44]. The maximum percentage removal of TOC reaches 78 % at 60 ° C.

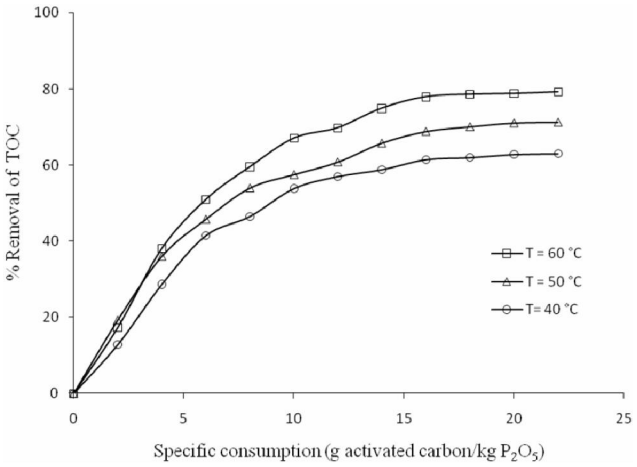

Figure 12 : Effect of specific consumption on the removal of TOC contained in Tunisian industrial phosphoric acid.

Comparison to commercially available adsorbent materials

Figure 13 provides a comparison of removal capabilitie for optimal activated carbon oxidized relative to commercial activated carbons designed for TOC removal. This figure shows that the tested commercial carbons have lower performance compared to the activated carbon oxidized. The removal of TOC onto three types of the activated carbon increases with time and then attains equilibrium value at a time of about 150 min.

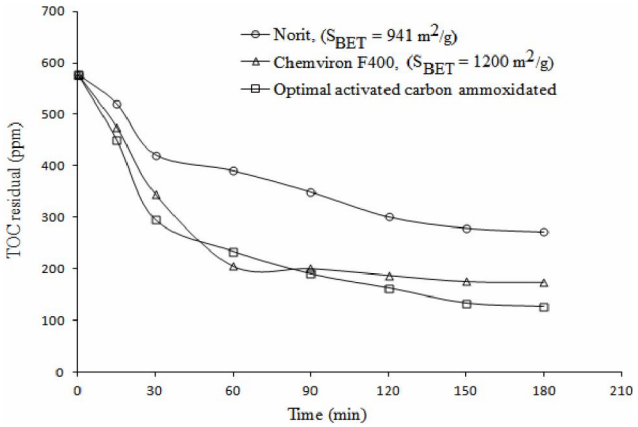

Figure 13 : A comparison of optimal activated carbon oxidized and commercial activated carbons

CONCLUSION

The results of this work demonstrate that almond shell is an attractive source of raw material for preparing high quality activated carbon by physical activation with carbon dioxide. The activation temperature and the activation time were found to have important influences on the development of the pore structure which caused increasing the iodine and methylene blue numbers of the activated carbon. The optimum activation temperature is 800 °C for 120 min activation time with under a 100 cm^3/ min carbon dioxide flow rate. Under these conditions, the largest BET surface area for the almond shell-activated carbon was 1310 m^2/ g. The optimal activated carbon was ammoxidated for increase the basicity of their surface in order to application for the removal of total organic carbon from Tunisian industrial phosphoric acid. In addition, adsorption times of 150 min and specific consumption to 16 g AC/kg P_2O_5 assure both steady state and maximum removal of total organic carbon.

ACKNOWLEDGEMENTS

The authors thank the Scientific Research Projects Unit of Valorization of the Useful Substances (ENIS) for the support of this work through the project. Also, I thank Mr. Bechir ELBEJAOUI for this linguistic assistance in this manuscript.

REFERENCES

[1] R.Baccar, J.Bouzid, M.Feki, A.Montiel; J.Hazard. Mater., **162**, 1522 **(2009)**.

[2] A.N.A.El-Hendawy; Appl.Surf.Sci., **252**, 287 **(2005)**.

[3] J.N.Sahu, J.Acharya, B.C.Meikap; J.Hazard. Mater., **172**, 818 **(2009)**.

[4] S.A.Dastgheib, A.R.David; Carbon, **39**, 1849 **(2001)**.

[5] I.A.W.Tan, A.L.Ahmad, B.H.Hameed; J.Hazard. Mater., **153**, 709 **(2008)**.

[6] D.Adinata, W.M.Ashri, M.K.Aroua; Bioresour. Technol., **98**, 145 **(2007)**.

[7] A.Namane, A.Mekarzia, K.Benrachedi, N.Bensemra, A.Hellal; J.Hazard.Mater., **119**, 189 **(2005)**.

[8] H.Hasar; J.Hazard.Mater., **B97**, 49 **(2003)**.

[9] N.Bagheri, J.Abedi; Chem.En.Res.Design, **87**, 1059 **(2009)**.

[10] W.T.Tsai, C.Y.Chang, S.L.Lee; Carbon, **35**, 1198 **(1997)**.

[11] Y.P.Guo, D.A.Rockstraw; Micropor.Mesopor. Mater., **100**, 12 **(2007)**.

[12] J.Hayshi, H.Toshihide, T.Isao, M.Katsuhiko, NA.Fard; Carbon, **40**, 2381 **(2002)**.

[13] M.Ahmedna, W.E.Marshall, R.M.Rao; Bioresour. Technol., **71(2)**, 113 **(2000)**.

[14] T.Y.Zhang, W.P.Walawender, L.T.Fan, M.H.Fan, D.Daugaard, R.C.Brown; Chem.Eng.J., **105**, 53 **(2004)**.

[15] T.Yang, A.C.Lua; J.Colloid.Interf.Sci., **267**, 408 **(2003)**.

[16] N.M.Haimour, S.Emeish; Waste Manage., **26**, 651 **(2006)**.

[17] B.G.P.Kumar, K.Shivakamy, L.R.Miranda, M.Velan; J.Hazard.Mater., **136**, 922 **(2006)**.

[18] M.Feki; Contribution to the Phosphoric-Acid Purification of Wet Process by Extraction with the Methyl-Isobutylcetone, Thesis, University of Sciences, Tunis, **(2001)**.

[19] B.S.Girgis, El-Hendawy, A.Abdel-Nasser; Micropor.Mesopor.Mater., **52**, 105 **(2002)**.

[20] T.Yang, A.Chong Lua; Mater.Chem.Phys., **100**, 438 **(2006)**.

[21] J.Starck, P.Burg, D.Cagniant, J.M.D.Tascon, A.Martinez-Alonso; Fuel, **83**, 845 **(2004)**.

[22] H.P.Boehm; Carbon, **32(5)**, 759 **(1994)**.

[23] A.Baçaoui, A.Yaacoubi, A.Dahbi, C.Bennouna, R.Phan Tan Luu, F.J.Maldonado-Hodar, J.Rivera-Utrilla, C.Moreno-Castilla; Carbon, **39**, 425 **(2001)**.

[24] A.C.Lua, T.Yang; J.Colloid Interface Sci., **274**, 594 **(2004)**.

[25] C.Bouchelta, M.S.Medjram, O.Bertrand, J.-P.Bellat; J.Anal.Appl.Pyrolysis, **82**, 70 **(2008)**.

[26] Q.Cao, K.C.Xie, Y.K.Lv, W.R.Bao; Bioresour. Technol., **97**, 110 **(2006)**.

[27] T.Yang, A.C.Lua; J.Colloid Interface Sci., **267**, 408 **(2003)**.

[28] A.M.Puziy, O.I.Poddubnaya, A.Martinez-Alonso, F.Suarez-Garcia, J.M.D.Tascon; Carbon, **40**, 1493 **(2002)**.

[29] L.J.Kennedy, J.J.Vijaya, K.Kayalvizhi, G.Sekaran; Chem.Eng.J., **132**, 279 **(2007)**.

[30] T.Yang, A.C.Lua; Mater.Chem.Phys., **100**, 438 **(2006)**.

[31] C.Pechyen, D.Atong, D.Ahtong, V.Sricharoenchaikul; J.Solid.Mech.Mater.Eng., **1**, 498 **(2006)**.

[32] A.Omri, H.Bel Haj Ltaief, M.Benzina; Environmental Science: An Indian Journal, (In press).

[33] B.Nasr, B.Hedi, G.Abdellatif, M.Rodrigo; Chem. Eng.Technol., **28**, **(2005)**.

[34] A.Mellah, A.Silem, R.Kada, A.Boualia; Can.J.Appl. Spectrosc., **36**, 94 **(1991)**.

[35] S.Biniak, G.Szymanski, J.Siedlewski, A.Swiatkowski; Carbon, **35**, 1799 **(1997)**.

[36] P.Vinke, M.van der Eijk, M.Verbree, A.F.Voskamp, H.van Bekkum; Carbon, **32**, 675 **(1994)**.

[37] M.Abe, K.Kawashima, K.Kozawa, H.Sakai, K.Kaneko; Langmuir, **16**, 5059 **(2000)**.

[38] J.R.Pels, F.Kapteijn, J.A.Moulijn, Q.Zhu, K.M.Thomas; Carbon, **33**, 1641 **(1995)**.

[39] S.A.Dastgheib, T.Karanfil, W.Cheng; Carbon, **42**, 547 **(2004)**.

[40] M.A.Montes-Morán, D.Suárez, J.A.Menéndez, E.Fuente; Carbon, **42**, 1219 **(2004)**.

[41] K.B.Bota, G.M.K.Abotsi; Fuel, **73**, 1354 **(1994)**.

[42] A.Sari, M.Tuzen, D.Citak, M.Soylak; J.Hazard. Mater., **148**, 387 **(2007)**.

[43] V.K.Garg, R.Kumar, R.Gupta; J.Dyes Pig., **62**, 1 **(2004)**.

[44] B.H.Hameed, M.I.El-Khaiary; J.Hazard.Mater., **154**, 237 **(2008)**.